Journal of Power Sources 195 (2010) 2830–2834

Contents lists available at ScienceDirect

Journal of Power Sources

journal homepage: www.elsevier.com/locate/jpowsour

Short communication

Characterization of hydrogen generation for fuel cells via borane hydrolysis using an electroless-deposited Co–P/Ni foam catalyst

KwangSup Eom, MinJoong Kim, RyongHee Kim, DoHwan Nam, HyukSang Kwon*

Department of Materials Science and Engineering, Korea Advanced Institute of Science and Technology, Guseong-dong 373-1, Yuseong-gu, Daejeon 305-701, Republic of Korea

ARTICLE INFO

Article history:
Received 8 September 2009
Received in revised form 6 October 2009
Accepted 13 November 2009
Available online 26 November 2009

Keywords:
Ammonia borane
Co–P/Ni foam catalyst
Fuel cell
Hydrogen
Durability
Electroless-deposition

ABSTRACT

The effect of an electroless-deposited Co–P/Ni foam catalyst on H_2 generation kinetics in ammonia borane (NH_3BH_3) solution and the cyclic behaviour (durability) of the catalyst are investigated. The electroless-deposited Co–P is composed of an inner flat layer and outer layer that consists of an aggregate of spherical particles. The H_2 generation rate/projected area of the Co–P/Ni foam catalyst is much higher than that of a Co–P/Cu sheet catalyst. The activation energy (E_a) for the hydrolysis of NH_3BH_3 using the Co–P/Ni foam catalyst is calculated to be 48 kJ mol^{-1}. After the first cycle, the H_2 generation rate decreases dramatically, i.e., by 16%, due to a decrease in surface area caused by the partial separation of spherical Co–P particles. Between the first and sixth cycles, the H_2 generation rate decreases gradually (by 14%) on account of a decrease in the number of P atoms that create active metallic Co sites on catalytic surface. After six cycles, about 70% of the initial H_2 generation rate remains constant. The study reveals a promising means of hydrogen generation for polymer electrolyte membrane fuel cells.

1. Introduction

Hydrogen has immense potential as a clean energy source for electric devices and vehicles because its chemical energy can be easily converted to electric energy by polymer electrolyte membrane fuel cells (PEMFCs). To ensure that PEMFCs function successfully using hydrogen, it is important to develop a convenient and safe H_2 storage and production system. In the past 10 years, on-board H_2 production methods for vehicles, for example, the hydrolysis of chemical hydrides such as $NaBH_4$, $LiBH_4$, NaH, $NaAlH_4$ and NH_3BH_3, have received much attention [1–22]. Specifically, ammonia borane (NH_3BH_3) can be dissolved stably in neutral water at room temperature. It can also produce a large amount of H_2 (8.96 wt.% H_2, stoichiometrically) via hydrolysis, according to:

$$NH_3BH_3 + 2H_2O \rightarrow NH_4^+ + BO_2^- + 3H_2 \quad (1)$$

To employ H_2 as a direct fuel supply for PEMFCs a suitable catalyst is needed to accelerate the hydrolysis of NH_3BH_3. From previous efforts, various catalysts with excellent catalytic performance have been developed [6–17]. These include not only noble metal based catalysts such as Pt, M/γ-Al_2O_3 (Ru, Rh, Pd, Pt and Au), PtM/C (M = Ir, Ru, Co, Cu, Sn, Au, and Ni), Ru/C, Ru/alumina, and Rh(0) nanoclusters [6–11], but also non-noble metal based catalysts [12–17] such as Ni and Co/γ-Al_2O_3, Ni and Co nanoparticles, Cu/Cu_2O, Poly(N-vinyl-2-pyrrolidone) (PVP) stabilized Ni, Ni-SiO_2 and Fe–Ni alloys. Unfortunately, most of the aforementioned catalysts, except for the magnetic Fe–Ni alloy catalyst [17], are difficult to use repeatedly in solution because they are in a powdery form or are supported weakly on a substrate. The development of catalysts with high durability is thus important for practical use.

Liu and Li [3] reported that increase in the volume of hydrogen causes a powerful shock on the catalyst support when a high H_2 generation rate is required. To solve this problem, some researchers [18–21] used porous Ni foam with a three-dimensional network structure as a substrate to absorb the shock. Catalytic materials such as Co/Ni powder, Co–B and Co–W–B were supported on the commercial Ni foam and it was found that the catalysts/Ni foam exhibited high durability. Moreover, the system yielded a high rate of hydrogen generation per projected area because Ni foam allows a large loading of catalytic material. We have reported that a Co–P catalyst electroless deposited on Cu sheet exhibits an excellent catalytic efficiency for hydrogen generation from an alkaline $NaBH_4$ solution [22]. Nevertheless, the H_2 generation kinetics and the durability of a Co–P catalyst electroless deposited on Ni foam in NH_3BH_3 solution have still to be elucidated. Present work involves an investigation of the effects of the Co–P/Ni foam catalyst on the H_2 generation kinetics of the hydrolysis of NH_3BH_3, together with the cyclic behaviour of the catalyst.

* Corresponding author. Tel.: +82 42 869 3326; fax: +82 42 869 3310.
E-mail address: hskwon@kaist.ac.kr (H. Kwon).

0378-7753/$ – see front matter © 2009 Elsevier B.V. All rights reserved.
doi:10.1016/j.jpowsour.2009.11.084

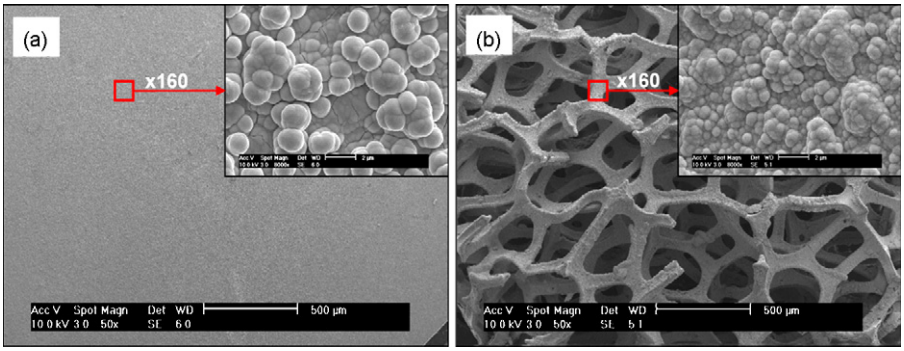

Fig. 1. Surface morphologies of (a) electroless-deposited Co–P on smooth Cu sheet and of (b) electroless-deposited Co–P on Ni foam with three-dimensional network structure.

2. Experimental

2.1. Preparation of catalysts

A Co–P/Ni foam catalyst was fabricated by electroless-deposition. The deposition was conducted on commercial Ni foam with a projected surface area of $1 \times 1\ cm^2$. The Ni foam has a three-dimensional open structure that is 1.6 mm thick and has pores of 0.1–0.5 mm in size. A smooth sheet of Cu (thickness: ~18 μm) was used as a point of comparison with Ni foam as the substrate material. The Ni foam was catalyzed in a $SnCl_2$ ($1\ g\ L^{-1}$) + HCl ($1\ ml\ L^{-1}$) solution for 3 min at 25 °C and accelerated in a $PdCl_2$ ($0.1\ g\ L^{-1}$) + HCl ($1\ ml\ L^{-1}$) solution for 1 min at 25 °C before undergoing electroless-deposition [22]. Electroless-deposition was performed for 3 min in a Co–P bath (0.1 M $CoCl_2{\cdot}6H_2O$, 0.6 M NH_2CH_2COOH and 0.8 M $NaH_2PO_2{\cdot}H_2O$) at pH 12.5 and 60 °C. These conditions were shown to be optimum for the fast generation of H_2 from the hydrolysis of $NaBH_4$ [22].

2.2. Characterization

The surface morphologies and compositions of the Co–P/Ni foam catalysts were analyzed by means of scanning electron microscopy (SEM) and energy dispersive spectroscopy (EDS). The structure and crystallinity of the catalysts were analyzed by X-ray diffraction (XRD). The electron bonding structures of the Co and P in the catalytic surface (~20 Å) of the Co–P/Ni foam catalyst were analyzed by X-ray photoelectron spectroscopy (XPS).

2.3. Determination of H_2 generation kinetics

To investigate the effects of the catalysts on the H_2 generation kinetics in NH_3BH_3 solution, H_2 generation tests were performed in 30 ml of 2 wt.% NH_3BH_3 (pH 9.0) solution at 30 °C in air. The volume of H_2 gas was measured by a water-displacement method using a buret. The reactor was immersed in a water bath to stabilize the temperature with no stirring in the reactor. The cycling test was conducted 15 times under the same conditions; each cycle consisted of immersion in the NH_3BH_3 solution for 1 h, rinsing for 10 s with deionized water, and drying for more than 5 h in a desiccator.

3. Results and discussion

3.1. Surface morphology and H_2 generation kinetics

Electroless-deposition of Co–P was conducted on a projected area of $1\ cm^2$ for both the Cu sheet and the Ni foam for 3 min at 65 °C in a Co–P bath. The weight of the Co–P deposit was $1.0\ mg\ cm^{-2}$ on the Cu sheet and $5.1\ mg\ cm^{-2}$ on the Ni foam. This indicates that Ni foam has a larger reactive surface area than a smooth Cu sheet. Fig. 1(a) shows the surface morphology of Co–P electroless deposited on a smooth Cu sheet, and Fig. 1(b) presents that of Co–P electroless deposited on the three-dimensional Ni foam. The Co–P deposited on a substrate is composed of both an outer layer of aggregated spherical Co–P particles and an inner flat layer that is 1 μm thick, as discussed previously [22]. From the EDS analysis, it is found that the Co–P deposited on Ni foam is composed of 8.4 wt.% P while Co–P deposited on a Cu sheet contains 8.9 wt.% P, indicating that the chemical compositions of the two different types of Co–P catalysts have little difference. The XRD patterns given in Fig. 2, have small broad peaks from Co (1 0 0) and Co (0 0 2), which confirm that nanocrystalline Co particles are precipitated in the amorphous Co–P structure, a phenomenon that was observed in TEM bright field images in a previous study [22]. The average size of the Co (0 0 2) particles in both the Co–P/Cu sheet catalyst and the Co–P/Ni foam catalyst was calculated using Scherrer's Formula and found to be 5.2 and 9.8 nm, respectively. The difference in average size of the Co particles between the two catalysts suggests that the catalytic activities (H_2 generation rate/catalyst weight) of the two catalysts may also be different. In our previous study [22], it was reported that the Co–P catalysts with smaller crystalline Co particles exhibited a higher catalytic activity in alkaline $NaBH_4$ solution. Thus, we expect the Co–P/Cu sheet catalyst with smaller Co nanoparticles to provide a higher rate of H_2 generation (per catalyst weight) in NH_3BH_3 solution.

To study the H_2 generation kinetics of both catalysts in NH_3BH_3 solution, a H_2 generation test was performed in 2 wt.% NH_3BH_3

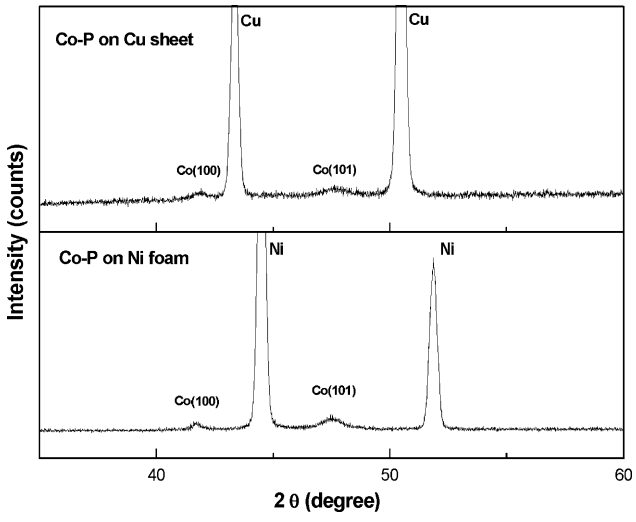

Fig. 2. XRD patterns of Co–P catalyst on (a) smooth Cu sheet and (b) Ni foam.

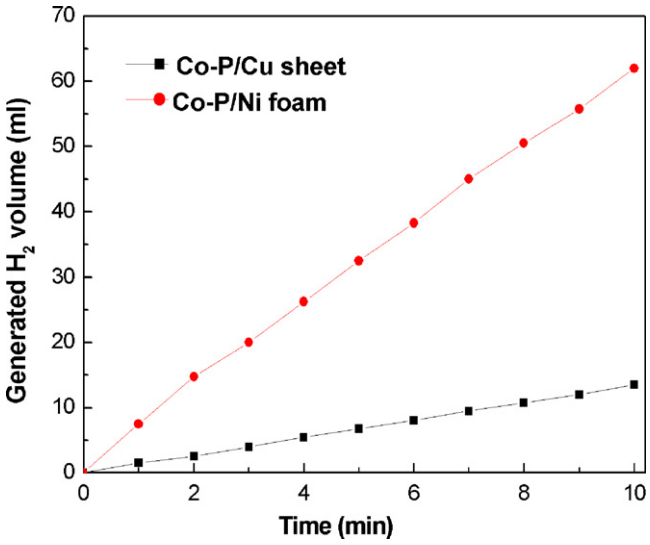

Fig. 3. Effects of Co–P/Cu sheet and Co–P/Ni foam catalysts on H_2 generation kinetics/projected catalyst area in 2 wt.% NH_3BH_3 solution at 30 °C.

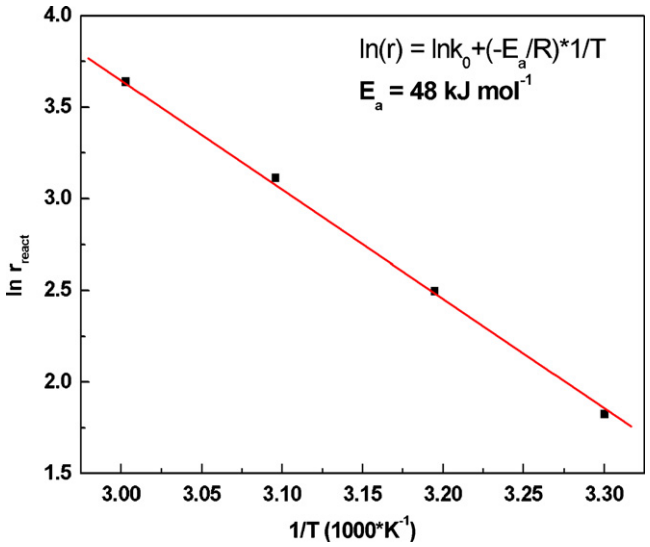

Fig. 5. $\ln r_{react}$ vs. $1/T$ plot for H_2 generation reaction using Co–P/Ni foam catalyst in 2 wt.% NH_3BH_3.

at 30 °C; the results are presented in Fig. 3. The H_2 generation rate/projected area of Co–P deposited on Ni foam is much higher (4.6 times) than that of the Co–P/Cu sheet catalyst. On the other hand, the H_2 generation rate per catalytic weight of the Co–P/Ni foam catalyst (1248 ml min^{-1} g^{-1}) is lower than that of the Co–P/Cu sheet catalyst (1350 ml min^{-1} g^{-1}). As discussed above, this is probably due to the difference in size of the precipitated nanocrystalline Co particles.

3.2. Catalytic activity (activation energy) of Co–P/Ni foam catalyst

The generation of hydrogen with a Co–P/Ni foam catalyst in 2 wt.% NH_3BH_3 solution at different temperatures from 30 to 60 °C is shown in Fig. 4. With increase in temperature, the H_2 generation rate of the Co–P catalyst dramatically increases from 6.2 to 38.1 ml min^{-1}. The initial H_2 generation reaction (0–10 min) can be considered to be of zeroth order because the H_2 generation rate is constant with reaction time. This indicates that the hydrolysis of NH_3BH_3 by the Co–P/Ni foam catalyst is not dependent on the concentration of NH_3BH_3 remaining in the solution. The reaction rate

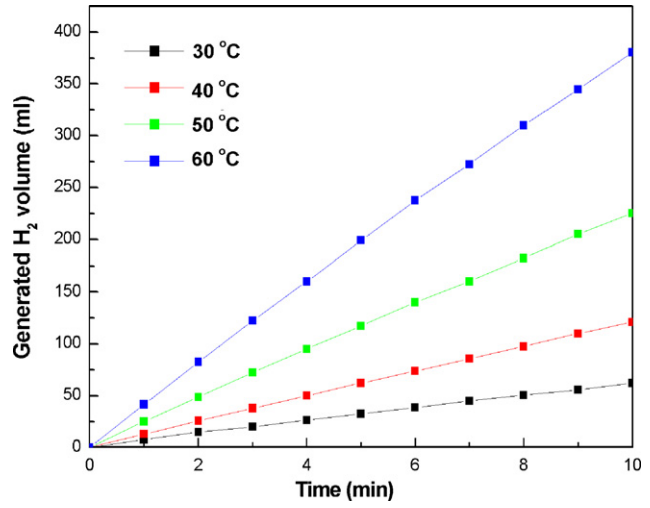

Fig. 4. Effects of NH_3BH_3 solution temperature on H_2 generation kinetics of Co–P/Cu sheet and Co–P/Ni foam catalysts in 1 wt.% NH_3BH_3 at 30, 40, 50 and 60 °C.

can be written as follows.

$$V_r = k_0 \exp\left(\frac{-E_a}{RT}\right) \quad (2)$$

where V_r is the reaction rate (ml min^{-1}); k_0 is the reaction constant (ml min^{-1}); E_a is the activation energy for the reaction; R is the gas constant; T is the reaction temperature (in kelvin). A $\ln V_r$ versus $1/T$ plot is given in Fig. 5 and is drawn using Eq. (2) and the data presented in Fig. 4. From the slope of the $\ln V_r$ versus $1/T$ plot, the activation energy (E_a) for the hydrolysis of NH_3BH_3 by the Co–P/Ni foam catalyst is calculated to be 48 kJ mol^{-1}. This value is higher than previously reported values for noble metal based catalysts, namely, Ru/γ-Al_2O_3: 23 kJ mol^{-1} [7], Rh/γ-Al_2O_3: 21 kJ mol^{-1} [7], Pt/γ-Al_2O_3: 21 kJ mol^{-1} [7], NiAg: 51.5 kJ mol^{-1} [9], but is much less than that for non-noble metal based catalysts (Co/γ-Al_2O_3: 62 kJ mol^{-1} [8]).

3.3. Durability performance of Co–P/Ni foam catalyst

The cyclic behaviour of the Co–P/Ni foam catalyst for H_2 generation from the hydrolysis of NH_3BH_3 is shown in Fig. 6. Each cycle entails employing the catalyst in a hydrolysis reaction for 1 h in 2 wt.% NH_3BH_3 at 30 °C, rinsing for about 10 s using deionized water and drying for more than 5 h in a desiccator. After the first cycle, the H_2 generation rate decreases markedly by 16%. Thereafter, from the second cycle to the sixth cycle, the H_2 generation rate gradually and steadily decreases by 14%. After the sixth cycle, about 70% of the initial H_2 generation rate remains, and the H_2 generation rate stays constant. The weight of Co–P remaining on the Ni foam following each cycle is plotted in Fig. 7. After the first cycle, the weight of Co–P decreases from 5.0 mg to 4.47 mg (a 10.6% drop). After the second cycle, however, the weight barely changes. A comparison of the morphologies presented in Figs. 8 and 1(b) reveals that, during the first cycle, some of the aggregated spherical Co–P particles in the inner layer separate, probably due to the expansion of H_2 volume sending powerful shocks through the catalyst support. The separation of some aggregated spherical Co–P particles may decrease the active surface area of the catalyst, thereby resulting in the dramatic reduction of the H_2 generation rate after first cycle. Because the catalytic weight does not decrease after the first cycle, however, other factors affecting the catalytic performance must exist. Nevertheless, the XRD pattern for the catalyst after the fifteenth cycle is found to be same as that for the catalyst before the first

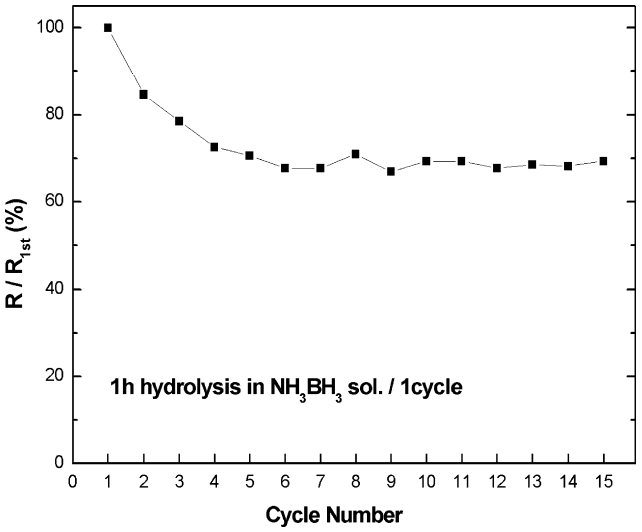

Fig. 6. Cycling behaviour of H_2 generation rate for Co–P/Cu sheet and Co–P/Ni foam catalysts (1 cycle: H_2 generation reaction for 1 h in 2 wt.% NH_3BH_3 solution).

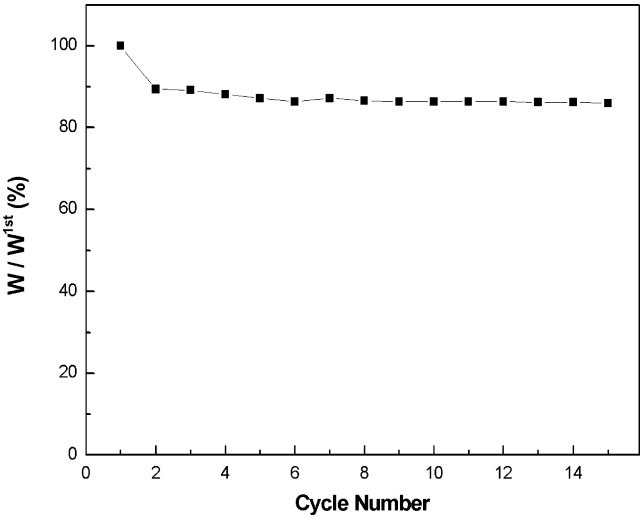

Fig. 7. Effect of cycling number on weight of Co–P/Ni foam catalyst in 2 wt.% NH_3BH_3 solution at 30 °C.

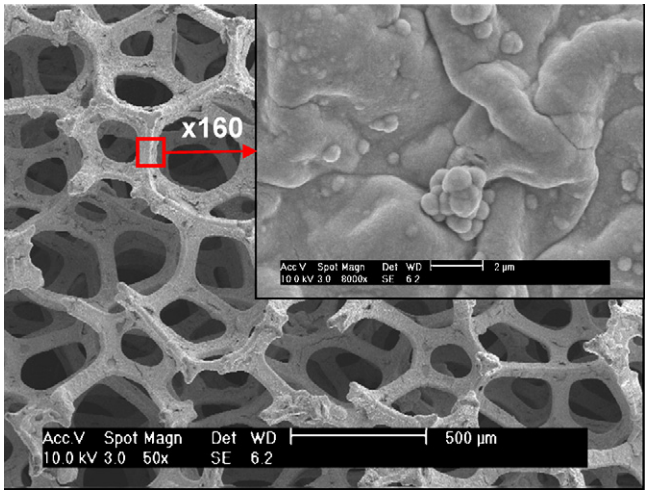

Fig. 8. Surface morphology of Co–P/Ni foam catalyst during cyclic testing (15 cycles = 15 h of hydrolysis).

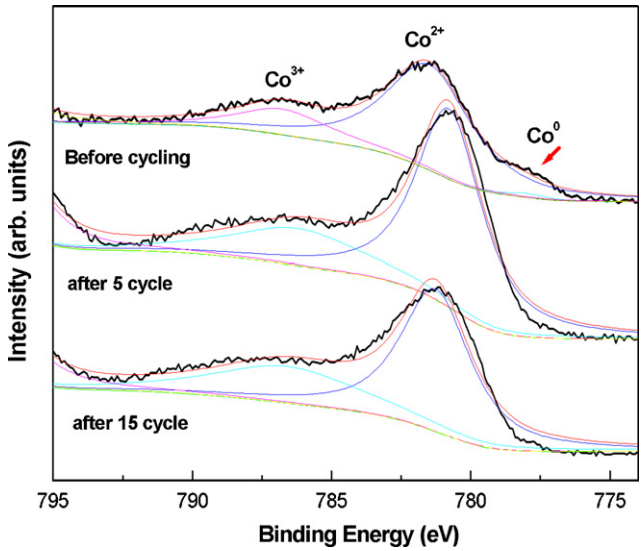

Fig. 9. XPS spectra of Co (probing the Co $^2P_{3/2}$ bonding orbital) in Co–P/Ni foam catalyst with cyclic testing.

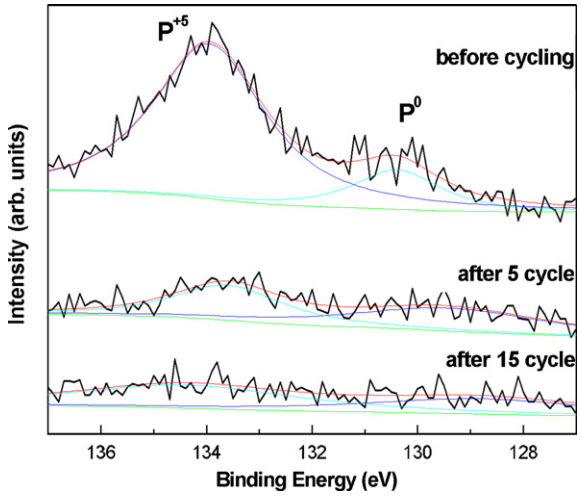

Fig. 10. XPS spectra of P (probing the P ^2P bonding orbital) in Co–P/Ni foam catalyst with cyclic testing.

cycling, thereby confirming no change in structure of the catalyst with cycling.

The XPS spectra of Co $^2P_{3/2}$ and P ^2P in the Co–P/Ni foam catalyst before and after the cyclic testing are shown in Figs. 9 and 10. Cobalt is composed of both metallic Co (Co^0) and oxidized Co (Co^{2+} and Co^{3+}) at the Co $^2P_{3/2}$ bonding orbital level and phosphorous consists of elemental P (P^0) and oxidized P (P^{5+}) at the P ^2P bonding orbital level. After the fifth cycle, of the large peak signifying oxidized Co (Co^{2+}) increases dramatically in amplitude and the small peak representing metallic Co (Co^0) almost disappears. The metallic Co does not completely oxidize because the oxidized Co peak shifts in the positive direction (into metallic Co) by 1 eV. After the fifteenth cycle, the peak shifts back in the negative direction (close to the oxidized Co). Meanwhile, the peaks signifying elemental P (P^0) and oxidized P (P^{5+}) both decreases dramatically as the number of cycles increases. As reported by Li et al. [23] and Patel et al. [24], P creates a high number of favourable active metallic Co sites for catalytic reaction. Therefore, from the present results, it is considered that active metallic Co sites decrease due to a decrease in the amount of P on the catalytic surface as well as the oxidation of metallic Co. Accordingly, between the first and sixth cycles, the H_2

generation kinetics of the Co–P/Ni foam catalyst might be gradually decreased. After six cycles, however the catalytic performance ceased to diminish. From SEM, XRD, and XPS analyses, this leveling off is due to a cessation in surface morphology changes.

4. Conclusions

The effect of an electroless-deposited Co–P/Ni foam catalyst on the H_2 generation kinetics in NH_3BH_3 solution, and the cyclic behaviour (durability) of the Co–P catalyst have both been investigated. The H_2 generation rate/projected area of Co–P deposited on Ni foam is much higher (4.6 times) than that of the Co–P/Cu sheet catalyst. The activation energy (E_a) for the hydrolysis of NH_3BH_3 using the Co–P/Ni foam catalyst is 48 kJ mol^{-1}. This value is higher than the previously reported value for noble metal based catalysts, but less than that for non-noble metal based catalysts. After the first cycle, the H_2 generation rate decreases dramatically (by 16%) due to a decrease in surface area by separation of the spherical Co–P particles. Between the first and sixth cycles, the H_2 generation rate decreases gradually (by 14%) due to a decrease in the number of P atoms that create active metallic Co sites. After the sixth cycle, 70% of the initial H_2 generation rate remains constant. Beyond six cycles, the H_2 generation performance of Co–P/Ni foam catalyst ceases to deteriorate.

Acknowledgement

This research was performed for the H_2 Energy R&D Center; one of the 21st Century Frontier R&D Programs funded by the Ministry of Science and Technology of Korea.

References

[1] H.I. Schlesinger, H.C. Brown, A.E. Finholt, J.R. Gilbreath, H.R. Hoekstra, E.K. Hyde, J. Am. Chem. Soc. 75 (1953) 215.
[2] S.C. Amendola, P. Onnerud, M.T. Kelly, P.J. Petillo, S.L. Sharp-Goldman, M. Binder, J. Power Sources 85 (2000) 186.
[3] B.H. Liu, Z.P. Li, J. Power Sources 187 (2009) 527.
[4] H.C. Kelly, V.B. Marriott, Inorg. Chem. 18 (1979) 2875.
[5] M. Chandra, Q. Xu, J. Power Sources 159 (2006) 855.
[6] M. Chandra, Q. Xu, J. Power Sources 156 (2006) 190.
[7] M. Chandra, Q. Xu, J. Power Sources 168 (2007) 135.
[8] Q. Xu, M. Chandra, J. Alloys Compd. 446 (2007) 729.
[9] C.F. Yao, L. Zhuang, Y.L. Cao, X.P. Ai, H.X. Yang, Int. J. Hydrogen Energy 33 (2008) 2462.
[10] S. Basu, A. Brockman, P. Gagare, Y. Zheng, P.V. Ramachandran, W.N. Delgass, J.P. Gore, J. Power Sources 188 (2009) 238.
[11] M. Zahmakıran, S. Özkar, Appl. Catal. B: Environ. 89 (2009) 104.
[12] Q. Xu, M. Chandra, J. Power Sources 163 (2006) 364.
[13] S.B. Kalidindi, M. Indirani, B.R. Jagirdar, Inorg. Chem. 47 (2008) 7424.
[14] S.B. Kalidindi, U. Sanyal, B.R. Jagirdar, Phys. Chem. Chem. Phys. 10 (2008) 5870.
[15] T. Umegaki, J.-M. Yan, X.-B. Zhang, H. Shioyama, N. Kuriyama, Q. Xu, Int. J. Hydrogen Energy 34 (2009) 3816.
[16] T. Umegaki, J.-M. Yan, X.-B. Zhang, H. Shioyama, N. Kuriyama, Q. Xu, J. Power Sources 191 (2009) 209.
[17] J.-M. Yan, X.-B. Zhang, S. Han, H. Shioyama, Q. Xu, J. Power Sources 194 (2009) 478.
[18] J.-H. Kim, H. Lee, S.-C. Han, H.-S. Kim, M.-S. Song, J.Y. Lee, Int. J. Hydrogen Energy 29 (2004) 263.
[19] J. Lee, K.Y. Kong, C.R. Jung, E. Cho, S.P. Yoon, J. Han, T.-G. Lee, S.W. Nam, Catal. Today 120 (2007) 305.
[20] H.-B. Dai, Y. Liang, P. Wang, H.-M. Cheng, J. Power Sources 177 (2008) 17.
[21] H.B. Dai, Y. Liang, P. Wang, X.D. Yao, T. Rufford, M. Lu, H.M. Cheng, Int. J. Hydrogen Energy 33 (2008) 4405.
[22] K.S. Eom, K.W. Cho, H.S. Kwon, J. Power Sources 180 (2008) 484.
[23] H. Li, P. Yang, D. Chu, H. Li, Appl. Catal. A: Gen. 325 (2007) 34.
[24] N. Patel, R. Fernandes, A. Miotello, J. Power Sources 188 (2009) 411.